

Modern Physics Letters A  
Vol. 21, No. 17 (2006) 1339–1353  
© World Scientific Publishing Company



## SEARCH FOR SINGLE TOP QUARK PRODUCTION AT DØ

REINHARD SCHWIENHORST

*Department of Physics and Astronomy, Michigan State University,  
East Lansing, MI 48824, USA  
schwier@pa.msu.edu*

Received 26 May 2006

We present a review of searches for electroweak production of single top quarks at the Fermilab Tevatron proton–antiproton collider at  $\sqrt{s} = 1.96$  TeV. Searches for  $s$ -channel and  $t$ -channel single top quark production have been carried out using secondary-vertex  $b$ -quark tagging and advanced event analysis methods in order to maximize the sensitivity to single top quark production. So far, no evidence for a single top quark signal has been found. However, 95% confidence level upper limits on the production cross-section have been set that improve upon previous limits by factors of two to three and are approaching the cross-section region predicted by the standard model.

*Keywords:* Top quark; single top; electroweak interaction; Tevatron.

PACS Nos.: 14.65.Ha, 12.15.Ji, 13.85.Qk, 87.18.Sn

### 1. Introduction

The top quark is by far the heaviest and most elusive fermion in the standard model (SM). Its large mass, and coupling strength to the Higgs boson of order unity, suggests a connection between the top quark and the physics of electroweak symmetry breaking (the origin of mass). In particular, the electroweak interaction of the top quark with the  $W$  boson is the key to predicting the Higgs boson mass within the SM. However, very little is currently known experimentally about the electroweak interaction of the top quark or the  $Wtb$  vertex. Significant advances in our understanding of the  $Wtb$  vertex can be made in the near future by studying the electroweak production of single top quarks at hadron colliders. In fact, observing and studying this interaction is one of the most important subjects for the Fermilab Tevatron proton–antiproton collider. Moreover, even before the observation of electroweak single top quark production, setting sufficiently tight limits on the production cross-section will serve to constrain several extensions to the SM that would enhance the single top quark production cross-section. A previous brief review focused on the search for single top quark production at the Tevatron at a center-of-mass energy of 1.8 TeV by the CDF collaboration.<sup>1</sup> This paper reviews

the first searches for single top quark production at the upgraded Tevatron at a center-of-mass energy of 1.96 TeV with the DØ detector which have now been completed.<sup>2,3</sup> These searches employ advanced analysis methods for optimized sensitivity, which set the stage for future searches on larger datasets. We present the single top quark final state at the parton level, review the current status of searches for single top quark production, focusing on a search using neural networks by the DØ collaboration. We also explore the potential for the discovery of this top quark production mode.

### 1.1. *Single top quark production*

The top quark was discovered by the CDF and DØ collaborations in 1995 at the Fermilab Tevatron proton–antiproton collider as top–antitop pairs.<sup>4,5</sup> The SM predicts that the top quark is also produced singly at hadron colliders through the electroweak charged current interaction, but this production process has not yet been observed. A measurement of the single top quark production cross-section will provide the first direct measurement of the CKM matrix element  $|V_{tb}|$ . Existing constraints on  $|V_{tb}|$  have been derived indirectly only, assuming three quark generations and unitarity of the CKM matrix.<sup>6</sup> Measuring the single top quark production cross-section provides a direct measurement because it is proportional to  $|V_{tb}|^2$ . The  $V - A$  structure of the top quark charged-current weak interaction can be probed in two ways: It can be tested directly in a study of spin correlations in single top quark events once this production mode has been observed. It can also be tested before single top quark production has been observed by combining limits on the single top quark production cross-section with measurements of the angular correlations of the top quark decay products in top quark pair events.<sup>7</sup> The single top quark final state is also predicted by several different models of new physics,<sup>8</sup> and studying single top quark production is a sensitive probe this new physics,<sup>8</sup> making it possible to rule out many extensions to the standard model even before reaching sensitivity to the standard model cross-section. It is furthermore a significant background to SM Higgs searches at the Tevatron in the associated production process  $q\bar{q}' \rightarrow WH$  with decay<sup>9–11</sup>  $H \rightarrow b\bar{b}$  and other new physics searches.<sup>12</sup> Finally, the experimental challenges encountered and analysis methods employed in the search for single top quark production can be applied directly to other searches at the Tevatron and the LHC, for example Higgs boson searches in the associated production and vector-boson-fusion channels.

Shown in Fig. 1 are the three possible SM single top quark production modes at hadron colliders. In the  $s$ -channel, a virtual  $W$  boson decays to a top quark and a bottom quark ( $t\bar{b}$ ). In the  $t$ -channel, a virtual  $W$  boson is exchanged between a light quark and a bottom quark, leading to a final state of a top quark and a light quark ( $tq$ ). Single top quarks are also produced in association with a  $W$  boson ( $tW$ ).

Of the single top quark production processes, the one with the largest production cross-section at the Tevatron at  $\sqrt{s} = 1.96$  TeV is due to the  $t$ -channel exchange,

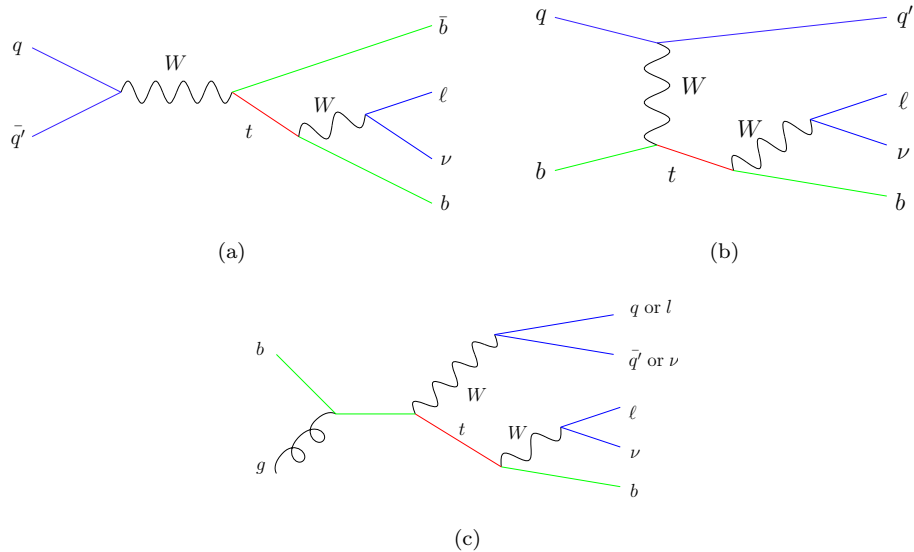


Fig. 1. Feynman diagrams for single top quark production and decay for (a)  $s$ -channel, (b)  $t$ -channel and (c) associated production.

for which calculations at next-to-leading order (NLO) in the strong coupling constant ( $\alpha_s$ ) yield a production cross-section of 1.98 pb.<sup>13,14</sup> The next largest cross-section is from the  $s$ -channel, for which NLO calculations predict a cross-section of 0.88 pb.<sup>13,14</sup> The associated production cross-section at the Tevatron is 0.1 pb,<sup>15</sup> which is too small to be observed.

### 1.2. Other collider searches for single top quark production

In Run I at the Tevatron, searches for single top quark production were performed by both the CDF and  $D\bar{O}$  collaborations. At the 95% confidence level, the limit by the CDF collaboration on the  $s$ -channel production cross-section is 18 pb, and the limit on the  $t$ -channel production cross-section is 13 pb.<sup>16</sup> The limit by the  $D\bar{O}$  collaboration on the  $s$ -channel production cross-section is 17 pb, and the limit on the  $t$ -channel production cross-section is 22 pb.<sup>17</sup> The CDF collaboration has also performed a search for a new heavy  $W'$  boson decaying to a top quark and a  $b$ -quark<sup>18</sup> and has set a limit of 533 GeV (566 GeV) if this quark is allowed to decay to leptons and quarks (only to quarks).

Single top quark production is kinematically possible at the LEP electron-positron and Hera electron-proton colliders as well. While the center-of-mass energy is not sufficient to produce top quark pairs at LEP, it is possible to produce single top quarks. Potential production modes at both colliders include flavor-changing neutral currents (FCNC) via photons or  $Z$  bosons. FCNC searches at LEP and Hera are complimentary and similar in sensitivity to those in the top quark decay

process.<sup>19</sup> The LEP and HERA experiments have found no evidence for single top quark production and set simultaneous limits on the FCNC couplings of the top quark to the photon and  $Z$  boson.<sup>20–25</sup>

The CDF collaboration has performed a search for single top quark production in Run II using  $170 \text{ pb}^{-1}$  of data.<sup>26</sup> The analysis maximizes the signal sensitivity and reduces the backgrounds as much as possible through a series of cuts on kinematic variables. A lepton (electron or muon) and missing transverse energy from the  $W$  boson decay are required, together with exactly two jets. At least one of the jets must be identified as a  $b$ -quark jet using a secondary-vertex based algorithm. Additional cuts on characteristic top quark event variables such as the reconstructed top quark mass are made to isolate single top quark events. The sensitivity of the analysis is improved beyond simple event counting by utilizing two distributions that show separation between the single top quark signal and the backgrounds: the pseudorapidity distribution of the light quark jet in the  $t$ -channel and the  $H_T$  distribution in the  $s$ -channel. Here,  $H_T$  is given by the scalar sum of the missing transverse energy and the transverse energies of the jets and leptons. No excess of events above the expected background from SM processes is found and limits are set on the single top quark production cross-sections of  $13.6 \text{ pb}$  in the  $s$ -channel and  $10.1 \text{ pb}$  in the  $t$ -channel.

## 2. Parton Level Distributions

This section discusses the final state signature of single top quark interactions at the parton level. The  $s$ -channel final state (Fig. 1(a)) consists of the lepton and neutrino from the  $W$  boson arising from the top quark decay, the  $b$ -quark from the top quark decay, and the  $\bar{b}$ -quark produced together with the top quark. The  $t$ -channel final state (Fig. 1(b)) consists of the same top quark decay products (lepton, neutrino,  $b$ -quark) and a light quark produced with the top quark. Furthermore, since the  $t$ -channel has an initial state  $b$ -quark, there is also a  $\bar{b}$ -quark produced from initial state radiation, although this quark typically appears at low transverse momentum and high pseudorapidity. It is also possible for one of the quarks to radiate off a gluon through either initial-state or final-state radiation. Similar to the  $\bar{b}$ -quark from gluon splitting in the  $t$ -channel, these radiated gluons typically have very low momentum.

Calculations have been performed at next-to-leading order in the strong coupling constant<sup>13,14,27</sup>  $\alpha_s$  that include the corrections to the top quark decay as well as preserve spin correlations.<sup>28–30</sup>

Figures 2 and 3 show the transverse energy ( $E_T$ ) and pseudorapidity<sup>a</sup> ( $\eta$ ) distributions of the final state jets, for both the  $s$ -channel and the  $t$ -channel. The events in these histograms have passed selection cuts similar to those used in the

<sup>a</sup>Pseudorapidity is defined as  $\eta = -\ln(\tan \frac{\theta}{2})$ , where  $\theta$  is the polar angle with origin at the interaction vertex.

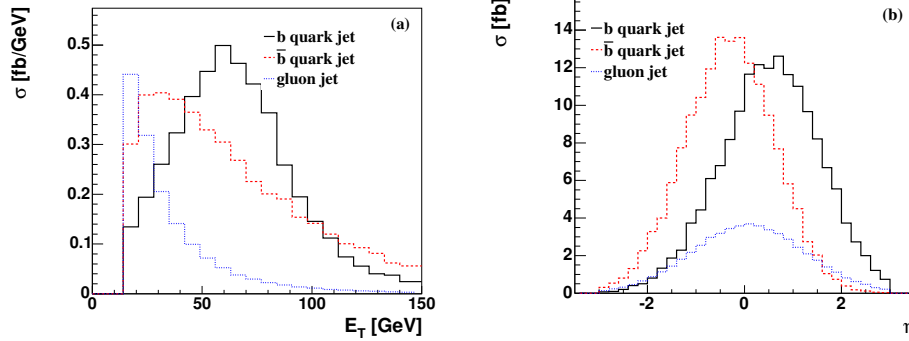


Fig. 2. Transverse energy (a) and pseudorapidity (b) distribution of final state jets at NLO for the  $s$ -channel, after selection cuts. Figure reprinted with permission from Q.-H. Cao, R. Schwienhorst, and C. P. Yuan, *Phys. Rev. D* **71**, 054023 (2005). © 2005 by the American Physical Society.

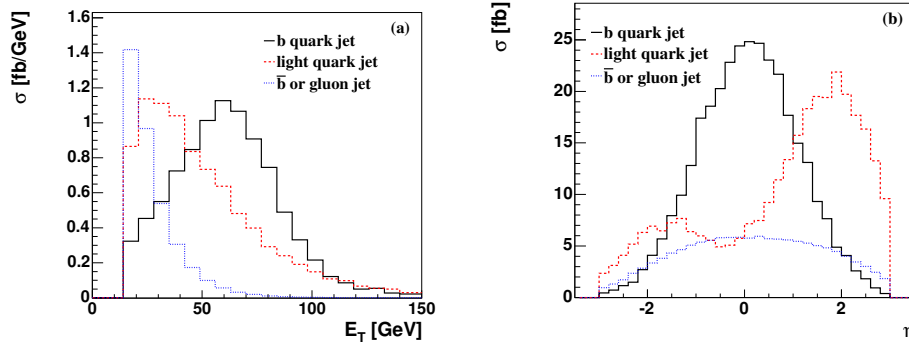


Fig. 3. Transverse energy (a) and pseudorapidity (b) distribution of final state jets at NLO for the  $t$ -channel, after selection cuts. Figure reprinted with permission from Q.-H. Cao, R. Schwienhorst, J. A. Benitez, R. Brock, and C. P. Yuan, *Phys. Rev. D* **72**, 094027 (2005). © 2005 by the American Physical Society.

experimental analysis below: requiring exactly one lepton with  $E_T > 15$  GeV, missing transverse energy  $\cancel{E}_T > 15$  GeV, and at least two jets with  $E_T > 15$  GeV. Only events in which a  $t$ -quark (not  $\bar{t}$ ) is produced are included in the plots, and only the electron decay mode of the  $W$  boson.

It can be seen from Fig. 2 that the  $s$ -channel final state jets all appear in the central pseudorapidity region, and that all, except for the gluon jet, are at high transverse energy. This gluon jet is not present at tree level but appears only in the  $O(\alpha_s)$  correction with real emission. About a third of the events in the  $s$ -channel contain such a jet for the given set of cuts.

Figure 3 shows the same kinematic distributions for the  $t$ -channel process. Again, the  $b$ -quark jet from the top quark decay appears at central rapidities and high  $E_T$ . The light quark jet, produced with the top quark, is also at high  $E_T$ , but it appears at more forward pseudorapidities, roughly following the initial state light quark. This large asymmetry produced by the proton-antiproton initial state is a

distinguishing feature of the  $t$ -channel process and can be used to separate it from the backgrounds. It can furthermore be combined with a smaller asymmetry in the pseudorapidity distribution of the charged lepton to maximize the sensitivity to  $t$ -channel single top quark production.<sup>31</sup> The additional radiation in the  $t$ -channel consists either of a gluon jet radiated off the  $b$  or light quark, or of a  $\bar{b}$ -quark jet from initial state gluon splitting into a  $b\bar{b}$ -quark pair, as shown in Fig. 1(b). This additional radiation is at low  $E_T$  and spreads out to higher pseudorapidities than the top quark decay products. About 40% of the  $t$ -channel events contain such an additional jet for the given set of cuts.

Figures 2 and 3 make it clear that in order to maximize the acceptance for single top quark events, the  $E_T$  and  $\eta$  cuts on the jets have to be kept as loose as possible. They also show, however, that at these low  $E_T$  thresholds, the  $O(\alpha_s)$  correction has a large impact on single top quark events and in particular, not only 2-jet events, but also 3-jet events should be included in the analysis.

### 3. Experimental Setup

The Tevatron in Run II is a 1.96 TeV proton–antiproton collider. The collider complex as well as the CDF and DØ detectors have undergone significant upgrades in preparation for Run II,<sup>32,33</sup> in particular the tracking<sup>34</sup> and trigger systems.<sup>35</sup> The DØ detector is comprised of tracking systems (silicon and fiber trackers in a magnetic field), electromagnetic and hadronic calorimeters, and a muon system. Data taking started in 2001 and is still ongoing. The analysis reviewed here is based on a dataset of 230 pb<sup>-1</sup>, collected with the DØ detector between 2001 and 2003. The Tevatron is expected to deliver between 4 fb<sup>-1</sup> and 8 fb<sup>-1</sup> by 2009.

### 4. Single Top Quark Event Selection

Single top quark signal-like events are selected containing a high- $E_T$  lepton (electron or muon), missing transverse energy  $\cancel{E}_T$ , and at least two jets. The event selection is designed to maximize the single top quark signal acceptance and to ensure that all backgrounds are well understood. The analysis comprises four analysis channels: separated by electron and muon from the  $W$  boson decay, as well as single- and double  $b$ -tagged events. While the selection cuts are similar for the  $s$ -channel and  $t$ -channel, the analysis is optimized independently for each of the two production modes.

In order to extract the single top quark signal from the large backgrounds, all detector elements need to be utilized so that the final state leptons and quark jets can be reconstructed precisely and with high efficiency. Events are selected by the trigger system if they contain an electron or muon plus at least one jet. Electrons and muons with high transverse energy ( $E_T > 15$  GeV) from the  $W$  boson decay are reconstructed in a detector pseudorapidity region of  $|\eta| < 1.0$  for electrons and  $|\eta| < 2.0$  for muons. Jets are reconstructed using a cone algorithm with a cone radius  $R = 0.5$ , where  $R = \sqrt{(\Delta\eta)^2 + (\Delta\phi)^2}$ ,  $\Delta\eta$  is the pseudorapidity difference and  $\Delta\phi$

the azimuthal angle difference between the two objects. Jets are identified efficiently if they have a transverse energy of more than 15 GeV and pseudorapidity  $|\eta| < 3.4$ . Such a larger pseudorapidity range is required to maximize the acceptance for the light quark jet in the  $t$ -channel, see Fig. 3(b). Electrons and muons are required to be isolated from jets by a distance of  $R > 0.5$ . Exactly one such isolated lepton is required in each event, as well as  $\cancel{E}_T > 15$  GeV to select a sample containing  $W$  bosons. Following the parton-level analysis presented above, events must have two, three, or four jets. with additional requirements for the leading jet of  $E_T > 25$  GeV and  $|\eta| < 2.5$ .

In order to suppress the large background from  $W + \text{jets}$  production,  $b$ -quark tagging is employed. The presence of a  $b$ -quark inside a jet is inferred from the presence of a displaced vertex due to the long lifetime of  $B$ -mesons and hadrons. The  $D\bar{O}$  detection efficiency to correctly identify a  $b$ -quark jet in a single top quark event is approximately 35%, and the mis-identification efficiency for a light quark jet is about 0.5%.<sup>36</sup> At least one of the jets is required to be  $b$ -tagged in each event. In addition, at least one non- $b$ -tagged jet is required in each event for the  $t$ -channel search.

These requirements (excluding  $b$ -tagging) select about 23% of the  $s$ -channel events and about 22% of the  $t$ -channel events (averaged over electrons and muons). The probability to find at least one  $b$ -tagged jet is 54% for the  $s$ -channel and 38% for the  $t$ -channel. The efficiency in the  $s$ -channel is higher than in the  $t$ -channel because of the presence of two high- $E_T$   $b$ -quark jets in the former.

#### 4.1. Event yields

There are several background processes that mimic the single top quark event signature. The dominant background that is hardest to beat down is from  $W$  boson production in association with jets. The second largest background contribution comes from  $t\bar{t}$  production, both in the lepton+jets and di-lepton decay modes. Smaller backgrounds are from QCD multijet production where one of the jets is mis-identified as an isolated lepton, and from di-boson events ( $WW$  and  $WZ$ ).

The event yields in each search after the selection cuts for the signals and backgrounds are listed in Table 1. Though there are expected to be a few single top quark events left after selection cuts, they are buried by the huge backgrounds. The signal to background ratio is 1:52 in the  $s$ -channel search and 1:32 in the  $t$ -channel search, making an extraction of the signal a daunting task.

The most important sources of systematic uncertainty on the signal acceptance are due to modeling of  $b$ -tagging and jet energy calibration. The largest uncertainty on the background normalization is due to the uncertainty in the theoretical cross-section or uncertainty in the normalization to data samples. The total uncertainty is about 15% for the signal acceptance and about 20% for the background normalization.

We can calculate 95% confidence level upper limits on production cross-section based on Table 1 to get an idea of the sensitivity of the analysis at this stage.

Table 1. Estimates for signal and background yields and the number of observed events in data passing the selection cuts. The total background for the  $s$ -channel ( $t$ -channel) search includes the background from  $t$ -channel ( $s$ -channel) production. Table reprinted with permission from V. M. Abazov *et al.*, *Phys. Rev. D* (2006). © 2006 by the American Physical Society.

	$s$ -channel search	$t$ -channel search
$s$ -channel	5.5	
$t$ -channel		8.5
$W$ + jets and di-boson	169	164
$t\bar{t}$	78	76
multijet	31	31
Total background	$287 \pm 44$	$276 \pm 41$
Observed events	283	271

Including systematic uncertainties, the limits on the production cross-section at the 95% confidence level (C.L.) are 13.0 pb in the  $s$ -channel and 13.6 pb in the  $t$ -channel. It is clear that in order to improve on these limits, we will have to go beyond event counting and need to take advantage of kinematic variables to separate the signals from the backgrounds.

## 5. Discriminating Variables

As the preceding section makes clear, further steps beyond event selection are required to extract the single top quark signals from the overwhelming backgrounds. In this section, we present important kinematic variables that separate the  $s$ -channel and  $t$ -channel signals from the backgrounds.

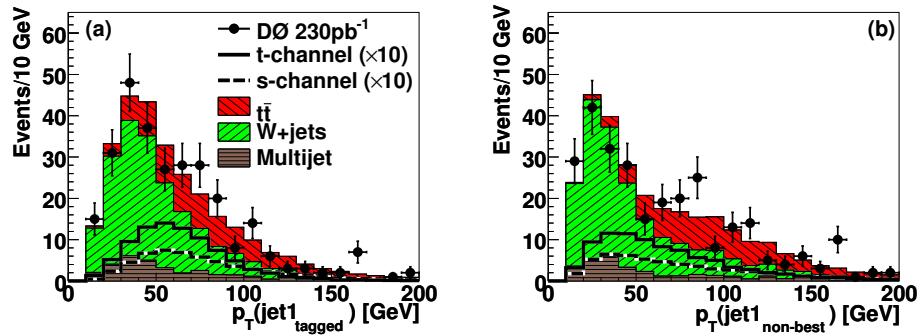


Fig. 4. Comparison of signal, background, and data for two important object kinematic variables. The figure shows (a) the transverse momentum of the leading  $b$ -tagged jet, and (b) the transverse momentum of the leading non-best jet. Signals are multiplied by ten for readability. Figure reprinted with permission from V. M. Abazov *et al.*, *Phys. Rev. D* (2006). © 2006 by the American Physical Society.

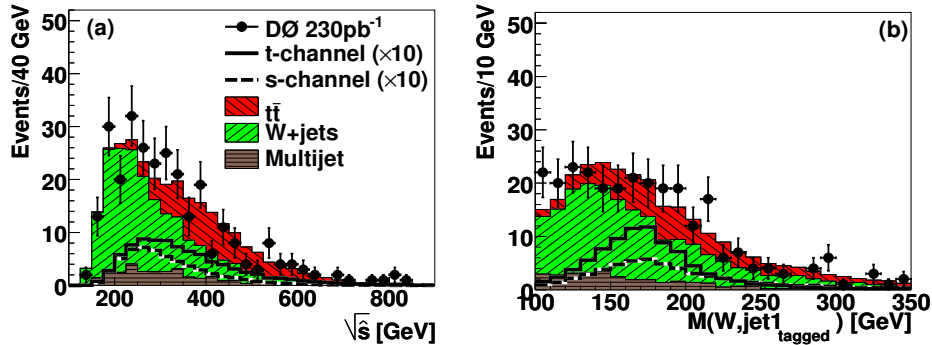


Fig. 5. Comparison of signal, background, and data for two important event kinematic variables. The figure shows (a) the invariant mass of all final state objects and (b) the invariant mass of the top quark reconstructed from the  $W$  boson and the leading  $b$ -tagged jet. Signals are multiplied by ten for readability. Figure reprinted with permission from V. M. Abazov *et al.*, *Phys. Rev. D* (2006). © 2006 by the American Physical Society.

To maximize the signal-background separation, the unique characteristics of the single top quark final state must be exploited. In particular, the dominant background from  $W + \text{jets}$  production does not contain a top quark in the final state. Thus specific properties of the top quark and its decay products are used, such as the large top quark mass, kinematic distributions of the top quark decay products, and top quark spin correlations. In order to do so, it is important to identify the decay products of the top quark in each event with high efficiency. The  $W$  boson is reconstructed from the isolated lepton and the missing transverse energy. The  $z$ -component of the neutrino momentum ( $p_z^\nu$ ) is calculated using a  $W$  boson mass constraint, choosing the solution with smaller  $|p_z^\nu|$  from the two possible solutions. The assignment of final state jets to either the  $b$ -quark from the top quark decay and the other quark is done differently for the  $s$ -channel and  $t$ -channel because of the different final state objects. In the  $s$ -channel analysis, the final state contains two high- $E_T$   $b$  quarks, and only one of them is typically identified through  $b$ -tagging. Thus,  $b$ -tagging information is not used in the  $s$ -channel to select the  $b$ -quark from the top quark decay. The top quark is instead reconstructed from the  $W$  boson and the “best” jet.<sup>17</sup> The best jet is defined as the jet in each event for which the invariant mass of the reconstructed  $W$  boson and jet is closest to  $m_t = 175$  GeV. The  $\bar{b}$ -quark produced together with the top quark is identified as the leading “non-best” jet.

In contrast to the  $s$ -channel, there is typically only one high- $E_T$   $b$ -quark in the  $t$ -channel final state, which is easily identified as the  $b$ -tagged jet. Thus, the top quark is reconstructed from the  $W$  boson and the leading  $b$ -tagged jet in the  $t$ -channel. The light quark is identified as the leading non- $b$ -tagged (or untagged) jet. Using these definitions, the  $b$ -quark jet originating from the top quark decay is correctly identified in about 90% of the single top quark signal events.

These reconstructed final state objects are utilized to define the discriminating variables, which fall into three categories: individual object kinematics (jet  $p_T$ ),

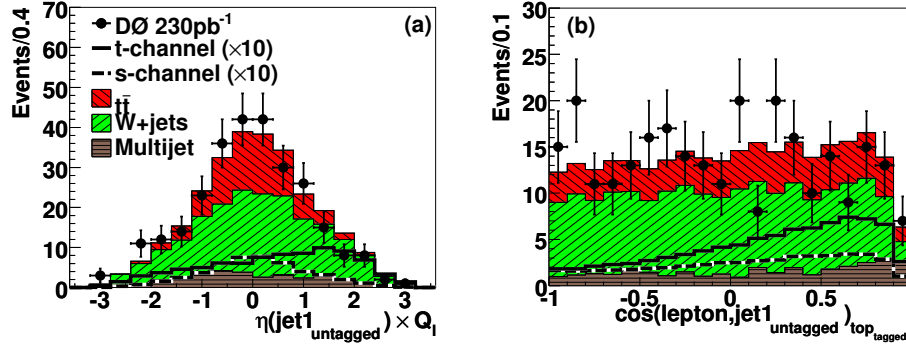


Fig. 6. Comparison of signal, background, and data for two important angular variables. The figure shows (a) the pseudorapidity of the leading untagged jet, corrected for the lepton charge, and (b) the angular correlation between the lepton and the leading untagged jet in the top quark rest frame. Signals are multiplied by ten for readability. Figure reprinted with permission from V. M. Abazov *et al.*, *Phys. Rev. D* (2006). © 2006 by the American Physical Society.

global event kinematics (reconstructed masses and sums of jet energies for various jet combinations), and angular correlations (jet angular separation and top quark spin correlations).

Two of the important individual object kinematic variables are shown in Fig. 4. They exploit the difference in jet  $E_T$  between the  $W$ +jets background, for which jets are typically at lower  $E_T$ , and the single top quark signals, for which jets are typically at higher  $E_T$ , see also Figs. 2(a) and 3(a).

These differences in individual jet energies are also reflected in global event kinematic variables such as the total energy or the total transverse energy  $H_T$  of various combinations of jets. Other global event kinematic variables take advantage of the presence of a heavy top quark in the final state, such as the invariant mass of the reconstructed top quark. Two of the important global event kinematic variables are shown in Fig. 5.

The top quark spin angular correlation variables rely in particular on the accurate reconstruction of the final state top quark, for example the top quark spin correlation in the optimal basis in the  $t$ -channel, shown in Fig. 6(a). Another important angular variable is the asymmetric pseudorapidity of the light quark in the  $t$ -channel, shown in Fig. 6(b) (see also Fig. 3(b)). Other angular variables exploit the difference in jet angles between the  $W$ +jets background (where jets from gluon splitting tend to be close together) and the single top quark signal (where jets tend to be well separated).

## 6. Optimized Event Analysis

No individual discriminating variable is sufficient to separate the single top quark signal from the backgrounds. Rather, they need to be combined in a multivariate analysis. Both the CDF and DØ collaborations have performed cut-based analyses in the past. In order to improve upon the sensitivity of these analyses, several

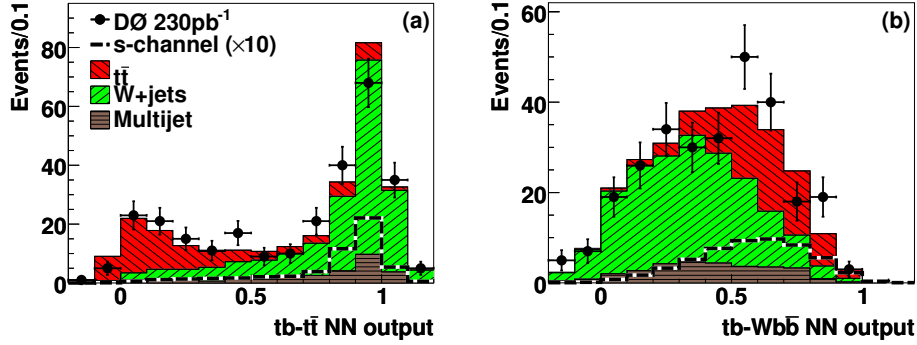


Fig. 7. Comparison of signal, background, and data for the neural network outputs for the  $s$ -channel ( $tb$ ) search. The figure shows the outputs for (a)  $tb-t\bar{t}$ , (b)  $tb-Wb\bar{b}$ . Signals are multiplied by ten for readability. Figure reprinted with permission from V. M. Abazov *et al.*, *Phys. Rev. D* (2006). © 2006 by the American Physical Society.

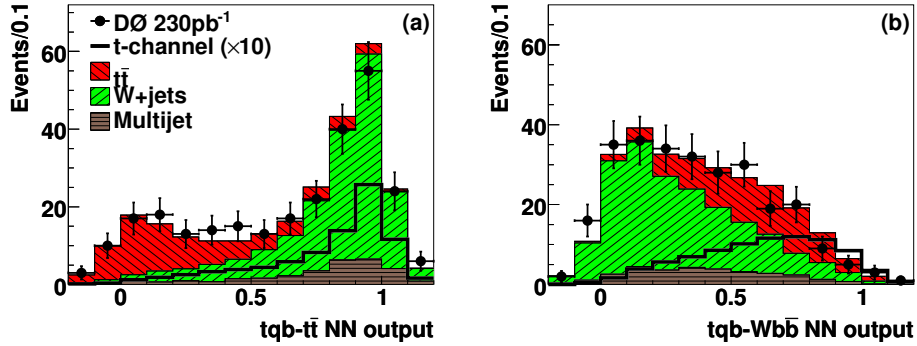


Fig. 8. Comparison of signal, background, and data for the neural network outputs for the  $t$ -channel ( $tqb$ ) search. The figure shows the outputs for (a)  $tqb-t\bar{t}$ , (b)  $tqb-Wb\bar{b}$ . Signals are multiplied by ten for readability. Figure reprinted with permission from V. M. Abazov *et al.*, *Phys. Rev. D* (2006). © 2006 by the American Physical Society.

event analysis methods<sup>1</sup> are in use by the  $D\bar{O}$  collaboration: neural networks,<sup>3</sup> likelihoods, and decision trees.<sup>37</sup> The different methods are based on the same set of discriminating variables and have been found to give similar sensitivity.

A total of 25 discriminating variables are combined in neural networks, optimized separately for the  $s$ -channel and the  $t$ -channel, and focused on separating the single top quark signals from the two largest backgrounds:  $W + \text{jets}$  and  $t\bar{t}$ . Each neural network has 11–13 input variables and is composed of three layers of nodes: an input layer, a hidden layer, and an output layer. The hidden layer typically has twice as many nodes as the input layer, and the output layer has exactly one node.

The output of the neural networks for the combined sample of electron and muon, single tagged and double tagged events, is shown in Fig. 7 for the  $s$ -channel, and in Fig. 8 for the  $t$ -channel. As expected, the neural networks are able to separate

the single top quark signals more effectively than any of the individual kinematic variables. Also, the networks separate signal and  $t\bar{t}$  backgrounds efficiently, but give less separation for  $W$ +jets, where the event kinematics are similar between signal and background.

Figures 7 and 8 show that the background model reproduces the data very well in the background-dominated region around neural network output values close to zero. They also show that there is no excess of events in the region close to one, indicating that there is no evidence for a single top quark signal.

The neural network output distributions also make the challenge posed by the different backgrounds clear: The  $W$ +jets ( $t\bar{t}$ ) background peaks in the signal region in the neural networks optimized for the  $t\bar{t}$  ( $W$ +jets) background. In order to optimize the sensitivity for the single top quark signal, both backgrounds need to be addressed simultaneously.

## 7. Statistical Analysis

The observed data are consistent with the background predictions for all analysis channels, and there is no evidence for a single top quark signal. Upper limits on the single top quark production cross-section are set, separately in the  $s$ -channel and  $t$ -channel searches using a Bayesian approach. In each search, two-dimensional histograms are constructed from the  $Wb\bar{b}$  versus  $t\bar{t}$  neural network outputs. A likelihood is built from these histograms for signal, background, and data, as a product over all channels (electron and muon, single and double tags) and all bins. A Poisson distribution is assumed for the observed number of events in each bin and a flat prior probability for the signal cross-section. The prior for the combined signal acceptance and background yields is a multivariate Gaussian with uncertainties and correlations described by a covariance matrix.

The Bayesian posterior probability densities are shown in Fig. 9 for both the  $s$ -channel and  $t$ -channel searches. The posterior density peaks at zero for the  $t$ -channel, indicating that there is no excess of data events over the background

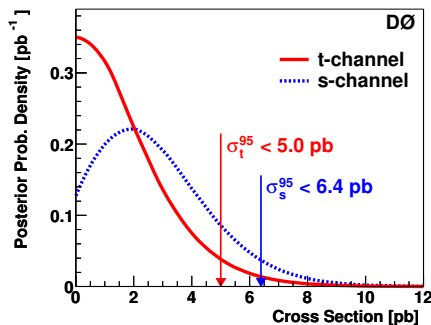


Fig. 9. The Bayesian posterior probability density as a function of the single top quark cross-section for the  $s$ -channel and  $t$ -channel searches. Figure reprinted with permission from V. M. Abazov *et al.*, *Phys. Lett. B* **622**, 265 (2005). © 2005 by Elsevier BV.

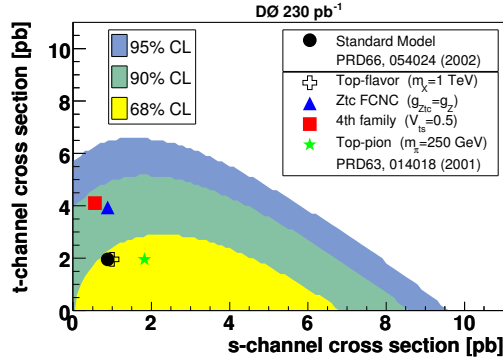


Fig. 10. Exclusion contours at 68%, 90%, and 95% confidence level on the posterior density distribution as a function of both the  $s$ -channel and  $t$ -channel cross-sections. Also shown are the SM single top quark production cross-sections as well as several representative new physics contributions. Figure reprinted with permission from V. M. Abazov *et al.*, *Phys. Rev. D* (2006). © 2006 by the American Physical Society.

sum. For the  $s$ -channel, the posterior density peaks at a value of around 2 pb, indicating that there is a small excess of data events over the background sum. However, the peak is very broad and less than one standard deviation away from zero, meaning that the data are also consistent with the background sum in the  $s$ -channel search. The corresponding upper limits on the production cross-sections at the 95% confidence level (C.L.) are 6.4 pb in the  $s$ -channel and 5.0 pb in the  $t$ -channel.

The sensitivity of these measurements is given by the expected upper limits, which are obtained by setting the observed number of events to the background prediction. The expected upper limits are 4.5 pb in the  $s$ -channel search and 5.8 pb in the  $t$ -channel search. The improvement in sensitivity compared to the limits after event selection is due to the use of a multivariate approach and shape information.

Since both the  $s$ -channel and  $t$ -channel searches are performed on the same dataset and probe similar physics, they can be combined in a single search. Figure 10 shows the posterior density as a function of both the  $s$ -channel and  $t$ -channel cross-sections, together with several possible models of new physics.<sup>8</sup> While none of these models are ruled out yet at the 95% confidence level, several of them are clearly disfavored compared to the SM. Dedicated searches, optimized for each new physics scenario, will be able to improve the sensitivity further, for example searches for  $W'$  boson production in the top quark decay channel.<sup>38</sup>

## 8. Summary

No evidence has been found so far for electroweak production of single top quarks in many searches at colliding beam machines. The most sensitive analysis to date has been performed by the  $D\bar{O}$  collaboration in  $230 \text{ pb}^{-1}$  of data collected at the Fermilab Tevatron proton-antiproton collider at a center-of-mass energy of

$\sqrt{s} = 1.96$  TeV. Upper limits at the 95% confidence level on the cross-section for the  $s$ -channel and  $t$ -channel processes have been set. The limits of 6.4 pb in the  $s$ -channel and 5.0 pb in the  $t$ -channel improve upon previously published limits by a factor of two and are approaching the region expected by the SM. In particular the  $t$ -channel limit is only a factor 2.5 above the cross-section value expected from the standard model.

Despite the increase data sample size compared to Run I at the Tevatron, the single top quark searches are still limited by statistical uncertainty. The sensitivity to SM single top quark production will improve as larger datasets are collected. The neural network analysis reviewed here will be sensitive to standard model single top quark production with a dataset corresponding to an integrated luminosity of around  $3 \text{ fb}^{-1}$ , proving that a discovery of single top quark production in Run II at the Tevatron is well within reach. This is the first time that an experimental analysis has reached the sensitivity required to be able to observe single top quark production in Run II. Moreover, datasets exceeding  $1 \text{ fb}^{-1}$  have already been collected by both the CDF and DØ collaborations and are currently being analyzed, and improvements are being made to all aspects of the analysis. As a result, sensitivity to SM single top quark production will likely be reached with datasets of  $2 \text{ fb}^{-1}$ , possibly even less. We are reaching the threshold of discoveries at the Tevatron and the next few years promise to be exciting times for top quark electroweak physics.

### Acknowledgments

We thank the DØ collaboration and in particular the single top working group and top physics groups and everyone else who contributed to the results reviewed here.

### References

1. C. I. Ciobanu and T. R. Junk, *Mod. Phys. Lett. A* **19**, 1493 (2004).
2. V. M. Abazov *et al.*, *Phys. Lett. B* **622**, 265 (2005).
3. V. M. Abazov *et al.*, submitted to *Phys. Rev. D* (2006).
4. F. Abe *et al.*, *Phys. Rev. Lett.* **74**, 2626 (1995).
5. S. Abachi *et al.*, *Phys. Rev. Lett.* **74**, 2632 (1995).
6. S. Eidelman *et al.*, *Phys. Lett. B* **592**, 1 (2004).
7. C. R. Chen, F. Larios and C. P. Yuan, *Phys. Lett. B* **631**, 126 (2005).
8. T. Tait and C.-P. Yuan, *Phys. Rev. D* **63**, 014018 (2001).
9. A. Stange, W. J. Marciano and S. Willenbrock, *Phys. Rev. D* **49**, 1354 (1994).
10. A. Stange, W. J. Marciano and S. Willenbrock, *Phys. Rev. D* **50**, 4491 (1994).
11. A. Belyaev, E. Boos and L. Dudko, *Mod. Phys. Lett. A* **10**, 25 (1995).
12. Q.-H. Cao, S. Kanemura and C.-P. Yuan, *Phys. Rev. D* **69**, 075008 (2004).
13. B. W. Harris, E. Laenen, L. Phaf, Z. Sullivan and S. Weinzierl, *Phys. Rev. D* **66**, 054024 (2002).
14. Z. Sullivan, *Phys. Rev. D* **70**, 114012 (2004).
15. J. Campbell and F. Tramontano, *Nucl. Phys. B* **726**, 109 (2005).
16. D. Acosta *et al.*, *Phys. Rev. D* **69**, 052003 (2004).

17. B. Abbott *et al.*, *Phys. Rev. D* **63**, 031101 (2001).
18. D. Acosta *et al.*, *Phys. Rev. Lett.* **90**, 081802 (2003).
19. F. Abe *et al.*, *Phys. Rev. Lett.* **80**, 2525 (1998).
20. A. Aktas *et al.*, *Eur. Phys. J. C* **33**, 9 (2004).
21. S. Chekanov *et al.*, *Phys. Lett. B* **559**, 153 (2003).
22. P. Achard *et al.*, *Phys. Lett. B* **549**, 290 (2002).
23. A. Heister *et al.*, *Phys. Lett. B* **543**, 173 (2002).
24. G. Abbiendi *et al.*, *Phys. Lett. B* **521**, 181 (2001).
25. J. Abdallah *et al.*, *Phys. Lett. B* **590**, 21 (2004).
26. D. Acosta *et al.*, *Phys. Rev. D* **71**, 012005 (2005).
27. J. Campbell, R. K. Ellis and F. Tramontano, *Phys. Rev. D* **70**, 094012 (2004).
28. Q.-H. Cao and C. P. Yuan, *Phys. Rev. D* **71**, 054022 (2005).
29. Q.-H. Cao, R. Schwienhorst and C. P. Yuan, *Phys. Rev. D* **71**, 054023 (2005).
30. Q.-H. Cao, R. Schwienhorst, J. A. Benitez, R. Brock and C. P. Yuan, *Phys. Rev. D* **72**, 094027 (2005).
31. M. T. Bowen, S. D. Ellis and M. J. Strassler, *Phys. Rev. D* **72**, 074016 (2005).
32. T. LeCompte and H. T. Diehl, *Annu. Rev. Nucl. Part. Sci.* **50**, 71 (2000).
33. V. Abazov *et al.*, accepted by *Nucl. Instrum. Meth. Phys. Res. A*, physics/0507191.
34. E. Kajfasz, *Nucl. Instrum. Meth. A* **511**, 16 (2003).
35. R. Schwienhorst, *Int. J. Mod. Phys. A* **20**, 3796 (2005).
36. V. M. Abazov *et al.*, *Phys. Lett. B* **626**, 35 (2005).
37. M. Narain, *PoS HEP2005*, 297 (2006).
38. M. Kopal, Top quark pair production and single top quark search at the Tevatron," *Proc. of the Rencontres de Moriond: EW Interactions and Unified Theories*, 2006.